

dolorg/10.15392/2319-0612.2025.2908 Braz. J. Radiat. Sci., Rio de Janeiro

2025, 13(4) | 01-19 | e2908 Editor: Prof. Dr. Bernardo Maranhão Dantas

Editor: Prof. Dr. Alfredo Lopes Ferreira Filho Submitted: 2025-04-25 Accepted: 2025-08-11



Automated dose-effect calibration curve for X-rays using the cytokinesis-block micronucleus assay

©Chaves-Campos*a,b,c F.A.; ©Ortíz-Moralesa,c F.; ©Cordero-Ramíreze,f, A.; ©Gómez-Castrod, J.; ©González-Mesac,g, J.E.

^aHealth Research Institute, University of Costa Rica. San José, Costa Rica.

bSchool of Health Technologies, University of Costa Rica. San José, Costa Rica.

^cLatin American Biological Dosimetry Network (LBDNet).

^dPhysics department, National University of Costa Rica., Heredia, Costa Rica.

eRadiotherapy Department. Hospital México. Costa Rican Social Security

Research Center in Materials Science and Engineering (CICIMA), University of Costa Rica, San José, Costa Rica

gCentro de Protección e Higiene de las Radiaciones (CPHR), Habana, Cuba.

*Correspondence: fabio.chavescampos@ucr.ac.cr

Abstract: This article shows the development of a dose-effect calibration curve for Xray exposures ranging from 0 to 4 Gy using the cytokinesis-block micronucleus assay and automated analysis—the first effort of its kind reported in Latin America. This work establishes a regional benchmark for high-throughput methodologies in cytogenetic biodosimetry, highlighting their potential to improve operational efficiency and reduce response times in radiological emergencies. Methods: Blood samples from six healthy donors were irradiated with X-rays at seven dose levels (0-4 Gy) using a calibrated 6 MV linear accelerator. Two blind samples (1.5 and 3 Gy) were included for validation. The CBMN assay was performed following IAEA protocols, DAPI-stained slides were analyzed using a AxioImager.Z2 automated microscope integrated with MetaSystems Metafer4 and the MNScoreX classifier software. A negative binomial regression model (NB1) was used for model fitting, accounting for overdispersion in micronucleus (MN) frequency. Results: Automated scoring of binucleated lymphocytes showed a dosedependent increase in MN frequency. The fitted model followed a linear-quadratic relationship: $Y = 0.0545 + 0.0448 \cdot D + 0.0145 \cdot D^2$, with all coefficients statistically significant (p < 0.001). Dose estimates for blinded samples (1.5 and 3 Gy) matched the true doses within 95% confidence intervals, with all z-scores < |3|. Conclusions: The resulting linear-quadratic dose-response curve enabled accurate estimation of blinded sample doses, with all z-scores falling within acceptable fitness-for-purpose thresholds. These results underscore the value of combining automated microscopy with robust statistical modeling to achieve reliable dose assessment, particularly in high-throughput settings and radiological emergency scenarios.

Keywords: biodosimetry, automation, micronucleus assay, radiation protection, radiation biology, radiological emergency.









doi org/10.15392/2319-0612.2025.2908 Braz. J. Radiat. Sci., Rio de Janeiro 2025, 13(4) | 01-19 | e2908

Editor: Prof. Dr. Bernardo Maranhão Dantas Editor: Prof. Dr. Alfredo Lopes Ferreira Filho

Submitted: 2025-04-25 Accepted: 2025-08-11



Curva de calibración dosis-efecto automatizada para exposiciones a rayos X utilizando el ensayo de micronúcleos con bloqueo de citocinesis

Resumen: Este artículo presenta el desarrollo de una curva de calibración dosis-efecto para exposiciones a rayos X en el rango de 0 a 4 Gy utilizando el ensayo de micronúcleos con bloqueo de citocinesis y análisis automatizado, siendo el primer esfuerzo de este tipo reportado en América Latina. Este trabajo establece un referente regional para metodologías de alta capacidad en biodosimetría citogenética, destacando su potencial para mejorar la eficiencia operativa y reducir los tiempos de respuesta en emergencias radiológicas. Métodos: Se irradiaron muestras de sangre de seis donantes sanos con rayos X en siete niveles de dosis (0-4 Gy) utilizando un acelerador lineal de 6 MV calibrado. Se incluyeron dos muestras ciegas (1.5 y 3 Gy) para validación. El ensayo CBMN se realizó siguiendo los protocolos del OIEA; las láminas teñidas con DAPI se analizaron utilizando un microscopio automatizado AxioImager.Z2 integrado con el sistema Metafer4 de MetaSystems y el software clasificador MNScoreX. Para el ajuste del modelo se empleó una regresión binomial negativa (NB1), que considera la sobredispersión en la frecuencia de micronúcleos (MN). Resultados: El análisis automatizado de linfocitos binucleados mostró un aumento dependiente de la dosis en la frecuencia de MN. El modelo ajustado presentó una relación lineal-cuadrática: $Y = 0.0545 + 0.0448 \cdot D + 0.0145 \cdot D^2$, con todos los coeficientes estadísticamente significativos (p ≤ 0.001). Las estimaciones de dosis para las muestras ciegas (1.5 y 3 Gy) coincidieron con las dosis reales dentro de los intervalos de confianza del 95%, y todos los puntajes z fueron < |3|. Conclusiones: La curva dosis respuesta sigue una función lineal-cuadrática, permitió una estimación precisa de las dosis en las muestras incógnitas, cumpliendo con los criterios de validación. Estos resultados destacan el valor de combinar microscopía automatizada con modelos estadísticos robustos para lograr evaluaciones de dosis confiables, especialmente como métodos de alto rendimiento y situaciones de emergencia radiológica.

Palabras clave: biodosimetría, automatización, ensayo de micronúcleos, protección radiológica, biología de las radiaciones, emergencia radiológica.









1. INTRODUCTION

Biological dosimetry (BD) encompasses a set of techniques used to assess exposure to ionizing radiation (IR) by analyzing biological markers of genetic damage. These methods allow the estimation of absorbed doses, evaluation of potential health risks, and the establishment of quantitative relationships between radiation dose and its biological effects. Such relationships are expressed through mathematical models and dose-effect curves, which are designed to predict the absorbed dose based on the analysis of specific biological endpoints following radiation overexposure [1]. One of the most widely implemented assays is the cytokinesis-block micronucleus (CBMN) assay, which is a complementary technique to the dicentric chromosomes assay (DC), the current gold standard technique in BD. The CBMN assay offers several advantages, including cost-effectiveness, simplicity, and rapid analysis, which collectively render it a versatile tool for use in BD laboratories [2]. The CBMN assay is frequently used as a general assay in toxicology; however, since radiation is a strong clastogenic agent for inducing micronuclei (MN), the CBMN assay has proven to be very reliable for assessing in vivo exposures, determining radiosensitivity, and susceptibility to cancer in vitro [1], [3]. Among the assay's disadvantages are the inherent variability in the baseline frequency of micronuclei, its limited performance in estimating doses for in vivo exposures of 0.2–0.3 Gy of X-rays, and its susceptibility to confounding variables. To address these limitations, several technical advancements have been proposed. For instance, recent developments combining imaging flow cytometry with AI-based image analysis have enabled fully automated MN scoring, offering high throughput and accuracy while overcoming many of the challenges associated with manual methods [4], [5].

Automated scoring of MN presents an opportunity to reduce the response times of BD laboratories while also mitigating subjective bias in the analysis. Implementing automated



microscopy systems enables the identification and classification of binucleated (BN) cells and MN, facilitates the measurement of morphological parameters, and enhances artifact elimination, thereby improving the accuracy and efficiency of analysis [6], [7].

Since the 1990s, different studies aimed at automating processes and analyses, have highlighted the use of systems for digitalizing slides through fluorescence microscopy and implementing optical density analysis modes, improving the differentiation between nuclei and MN. Subsequent aspects, such as the discrimination between nuclear and cytoplasmic material, recognition of main nuclei, area measurements, DNA content, and the morphological parameters of micronuclei, improved the sensitivity of the assays [8], [9]. In the following decade, new studies evaluated the capability of automated microscopy systems and computer image processing for scoring MN. In terms of reproducibility, the system demonstrated performance at least comparable to that of experienced human observers with several years of expertise in cytogenetics [10].

Subsequent analyses sought improvements through commercial software and workstations, such as Pathfinder LightVision, CELLSCAN [11] and Metafer [12], [13]; enabling mass evaluation of samples, reducing secondary validations (related to verifying the accuracy of results), minimizing artifacts, and increasing population triage (selecting and classifying individuals based on, for example, exposure to risk factors).

At the Central American level, our laboratory has published a semi-automated dose-response calibration curve for high X-ray doses using the PCCr assay, incorporating automated microscopy for the scanning of cell spreads [14]. This, together with interlaboratory exercises conducted through the Latin American Biological Dosimetry Network (LBDNet) using the dicentric chromosome assay with semi-automated analysis, demonstrates the growing regional implementation of automated methods in BD [15].

This study describes the development of a dose–effect calibration curve for X-ray exposures (0–4 Gy) using the cytokinesis-block micronucleus (CBMN) assay combined



with automated microscopy—representing the first report of its kind in Latin America. At the regional level, it establishes a benchmark for high-throughput approaches in BD, highlighting their potential to improve efficiency and substantially reduce response times in radiological emergencies.

2. MATERIALS AND METHODS

2.1. Collection and irradiation of blood samples.

Seven individual 5 mL blood samples were collected in heparinized Vacutainer tubes from each of the six participants (three males and three females), all of whom provided informed consent. The samples were then irradiated at seven different doses (0, 0.25, 0.5, 1, 2, 3, and 4 Gy). To validate the calibration curve, two blind dose estimations were performed. For this purpose, two additional samples were irradiated with 1.5 Gy and 3 Gy, respectively, and coded as X and Y. The actual doses were concealed from the analysts.

For sample irradiation, a linear accelerator UNIQUE from Varian Medical Systems (CA, USA) was used and calibrated according to the IAEA Technical Report No. 398 recommendations [16]. A 6 MV photon beam was set to deliver a dose rate of 1 cGy/MU at 90 cm SSD and a depth of 10 cm in water. A 30 cm \times 30 cm water phantom (PTW, Freiburg, Germany) was used, with samples placed on a central support located 15 cm from each lateral wall and immersed in water maintained at 37 \pm 0.5 °C, filled to 80% of the phantom's capacity. Irradiation was carried out using the Source-Axis Distance (SAD) technique with two opposing lateral fields oriented at 90° and 270°, each measuring 10 \times 10 cm. Equation 1 presents the calculation of the monitor units (MU) for each field; note that field heterogeneity was not taken into account in this calculation and subsequent analyses.

$$MU = \frac{D(cGy)}{D\pi, Ref * S_c(r_c) * S_p(r_d) * TMR(d, r_d) * F_{wedge} * F_{tray} * F_{OAR(d, x)}} * \left(\frac{SPD}{SAD + d_{max}}\right)^2 \quad (1)$$



Where the factors described in the equation are:

D(cGy): Desired dose value,

 $D\pi$, Ref: Reference dose per monitor unit under standard conditions,

 $S_c(r_c)$ Collimator calibration factor,

 $S_p(r_d)$: Phantom scatter factor,

TMR(d,r_d): Product of the attenuation factors by effective pathway and effective length,

Fwedge: Correction factor for the use of a wedge,

Ftray: Attenuation factor for reference collimation trays,

 $F_{OAR(d,x)}$: Correction factor for the off-center ratio,

SPD: Source-to-Phantom Distance,

SAD: Source-to-Axis Distance,

d_{max}: Depth of maximum dose,

For dose verification, Gafchromic EBT-XD films (lot 10172301; Ashland Specialty Ingredients G.P., Bridgewater, NJ, USA) were irradiated in the same position as the sample. The calibration curve for the EBT-XD films was established using a procedure that correlates optical density (OD) measurements with the dose delivered by the X-ray machine, ensuring traceability of the administered dose[17].

For a nominal sample dose of 3 Gy, three independent film measurements yielded dose values of 3.20 Gy, 3.11 Gy, and 3.19 Gy. Compared to the reference dose of 3.08 Gy, these values correspond to relative errors of 3.98%, 0.85%, and 3.88%, respectively. Dose verification errors below 5% are considered acceptable according to international recommendations [18].



A portable incubator model INB-203M Portable CO₂ (IKS International, NL) was employed to ensure temperature stability of blood samples post-irradiation and during transportation between centers. Following irradiation, the samples were incubated at 37 \pm 0.5°C for approximately two hours, providing adequate time for activation of cellular DNA damage response mechanisms.

The research protocol underwent scrutiny and received approval from the Scientific Ethical Committee of the University of Costa Rica (Project code C1-312). Before proceeding with sample collection, thorough explanations regarding donor participation and the intended utilization of the samples were provided. All personal information was anonymized, with coding procedures exclusively accessible to the principal investigator.

2.2. Cytokinesis Block Micronucleus Assay

Lymphocyte culture, cell harvesting, preparation of chromosome spreads, and cytogenetic analysis were performed according to the protocol described by the IAEA [3].

Initially, a volume of 0.5 mL of whole blood from each sample was added into conical tubes, each containing 4.5 mL of PBMax culture medium (Gibco brand) supplemented with Phytohemagglutinin (PHA) at a concentration of 3%. The tubes were then incubated at 37°C in a 5% CO₂ atmosphere for 72 hours.

After 24 hours of culture, cytochalasin B (Cyt-B) (Sigma) was added at a final concentration of 6 µg/mL from a 2 mg/mL stock solution prepared in DMSO (Merck).

Cells are harvested 3 days after the start of the culture (72 hours), and the cultures are centrifuged at 1200 RPM for 10 min to remove the supernatant. The cell pellet was resuspended and treated with 7 ml of KCl (0.075 M) (MerK) at 4 °C and homogenized by inversion. The supernatant was removed, and 5 mL of freshly diluted fixative (methanol:acetic acid [10:1]) in a 1:1 ratio with Ringer's solution (4.5 g NaCl, 0.21 g KCl, 0.12 g CaCl₂ in 500 mL H₂O) was added. The cell suspension was vortexed to prevent clumping.



Subsequently, the cell pellet underwent at least three fixations using freshly prepared cold fixative until a whitish appearance was observed. During the final fixation, the supernatant was carefully removed, leaving approximately 1 mL of liquid above the pellet. The cells were then gently resuspended, and 25 µL of the suspension was carefully transferred onto clean microscope slides using a fixed-volume pipette. The slides were air-dried before being stained with Vectashield DAPI solution (Merck).

2.3. Microscopic analysis

The image capture process was performed using a Carl Zeiss AxioImager.Z2 automated microscope, equipped with MetaSystems Metafer4 software (Version 4.3.7). Automated analysis was conducted using the MNScoreX Classifier (Version 4.3.7), which considers specific criteria to classify an object as a BN cell. For example, a cell is considered BNwhen it contains two nuclei of similar shape, separated by a maximum absolute distance of 250 (measured in 1/10 µm). The complete set of parameters (classifier) used by the software to identify BN cells and MN is provided in Supplementary Document S1. Following image analysis, the distribution of BN cells by number of MN and the total MN count per dose were recorded. For doses of 0, 0.25, 0.5, and 1 Gy, a minimum of 2,000 BN cells per sample were analyzed. For doses above 1 Gy, at least 1,000 BN cells were scored per case.

2.4. Statistical analysis

The statistical data processing for calibration curve fitting, estimation of unknown doses, calculation of dispersion statistics for calibration fit, and graphical analysis were conducted using BioDose Tools and R scripts running on Rstudio [19], [20]. To test the goodness of fit to Poisson distribution and Negative Binomial distribution the U-test and Stein-type test were applied [21]. To model the relationship between radiation dose and MN frequency, a negative binomial regression model (NB1) was used. This approach accounts for overdispersion in the data, where the variance exceeds the mean. Model selection was based on the Akaike Information Criterion (AIC), residual deviance, and the



significance of estimated coefficients. For the unknown doses, the criterion for acceptance was that the estimated dose by biological dosimetry should not deviate by more than 20% from the dose determined by physical dosimetry [22].

3. RESULTS AND DISCUSSION

Automated microscopy systems, integrated with advanced pattern recognition software, have become increasingly prevalent in BD laboratories. These technologies facilitate the digitization of entire cell slides, enabling the automated identification of cells and chromosomal aberrations, and generating comprehensive reports on biomarker frequency analysis. By constructing dose-response curves based on these automated analyses, the process is expedited, ensuring consistent and reliable results.

A significant advantage of automated analysis is its potential to reduce inter-analyst variability in identifying DNA damage biomarkers. Traditional manual scoring methods are subject to subjective interpretations, leading to inconsistencies between different analysts. Automated systems standardize the identification process by applying uniform criteria across all samples, thereby minimizing subjective bias and enhancing reproducibility.

Table 1 summarizes the frequency of MN observed at increasing doses of X-ray irradiation, along with the total number of BN cells analyzed and the calculated dispersion statistics. The data reveal a marked dose-dependent increase in MN frequency, with higher doses leading to greater numbers of micronuclei per cell.

The mean number of MN per BN cell increases from 0.0485 at 0 Gy to 0.4746 at 4 Gy, reflecting a progressive accumulation of chromosomal damage with radiation dose. In parallel, the variance also rises, from 0.0522 at 0 Gy to 0.5293 at 4 Gy, indicating not only increased MN counts but also greater heterogeneity in the cellular response to irradiation.



As the dose increases, there is a marked rise in the proportion of BN cells containing two or more MN. At 0 Gy, only 6.7% of MN-positive cells exhibit more than one MN, whereas this figure rises to over 36% at 4 Gy. This trend supports the notion that higher radiation doses induce not only more frequent but also more severe chromosomal damage within individual cells.

Table 1: MN Frequency across X-ray doses

Cell distribution according to the number of													
Dose (Gy)	BN	MN			mic	ronucle	ei						
			0 MN	1 MN	2	3	4	5	6	mean	var	DI	U
					MN	MN	MN	MN	MN	incan			
0	14828	719	14154	629	45	0	0	0	0	0.0485	0.0522	1.0768	6.61
0,25	14793	1090	13815	877	94	4	2	1	0	0.0737	0.0856	1.1613	13.87
0,5	15727	1249	14611	1000	103	11	1	0	1	0.0794	0.0931	1.1721	15.26
1	13807	1702	12363	1239	167	25	11	2	0	0.1233	0.1556	1.2622	21.80
2	7833	1329	6691	984	133	22	2	1	0	0.1697	0.1973	1.1631	10.207
3	8379	2741	6290	1530	475	75	9	0	0	0.3271	0.4001	1.2232	14.447
4	7226	3429	4648	1865	594	102	16	0	1	0.4745	0.5292	1.1153	6.93

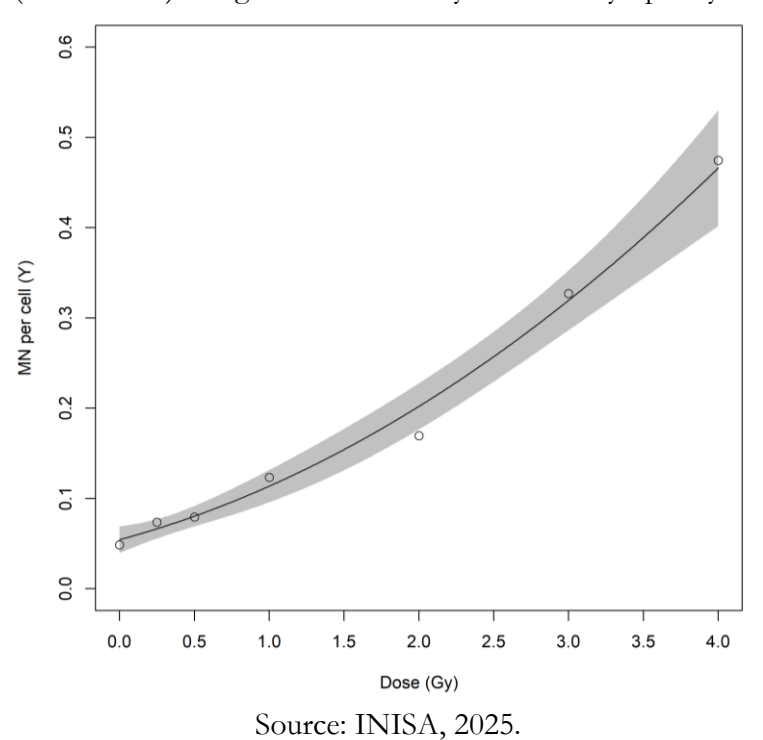
Although MN formation is often modeled under the assumption of a Poisson distribution, analysis of the dispersion index (DI) and U statistic reveals substantial overdispersion across the dose range.

These deviations from the Poisson model justify the use of a negative binomial regression (NB1), which accommodates overdispersion by allowing the variance to increase linearly with the mean. The NB1 model was identified as the most appropriate for these data, exhibiting improved fit metrics—including lower residual deviance, reduced Akaike Information Criterion (AIC), and higher log-likelihood—when compared to the Poisson and NB2 models. Furthermore, all model coefficients were statistically significant (p < 0.01), reinforcing the robustness of the fitted model for characterizing the dose–response relationship.



The resulting dose–response curve (Fig. 1) was derived from data obtained through automated analysis of 82,593 BN human lymphocytes exposed to X-rays across seven dose points. The frequency of MN (Y) exhibited a clear linear–quadratic relationship with the absorbed dose (D), consistent with the expected biological response to ionizing radiation.

Figure 1. Dose-response curve for MN at different X-rays doses (circle dots) with 95% confidence limits (shaded area) using the CBMN assay in human lymphocytes.



The resulting equation from this analysis is as follows:

 $Y = (0.054458 \pm 0.005267) + D \times (0.044763. \pm 0.012431) + D^{2} \times (0.014543. \pm 0.003736).$

To validate the curve, estimation for two unknown doses was conducted. The samples were irradiated homogeneously at 1.5 and 3 Gy, with the irradiation and lymphocyte culture conditions for the unknown sample being identical to those used to generate the calibration curve. Table 3 shows the estimated coefficients of the calibration curve with standard errors (SE).



Table 3. Summary of the NB1 model fit (Negative Binomial Type 1) for MN frequency as a function of radiation dose.

Coefficier	nt Estimate Sta	andard Error (Sl	E) z value p-value
С	0.054458	0.005267	$10.340 < 2e^{-16}$
α	0.044763	0.012431	3.601 0.000317
β	0.014543	0.003736	3.893 9.9e ⁻⁰⁵

In BD, two primary approaches are employed for estimating radiation doses using the CBMN assay: full analysis and triage analysis. Routine or full Analysis involves the evaluation of a larger number of BN cells, typically 1,000 or more per case. The extensive data collected allows for precise dose estimation, making it suitable for detailed assessments. However, the process is time-consuming and requires significant resources, which may not be practical in radiological emergencies. In contrast, triage analysis is designed for rapid assessment, particularly useful during mass-casualty incidents. It involves scoring a smaller number of BN cells, often around 200 per case. While this approach sacrifices some precision, it significantly reduces analysis time, enabling quicker decision-making. Studies have demonstrated that triage analysis can effectively identify individuals exposed to radiation doses ≥1 Gy, which is critical for immediate medical interventions [23], [24]. The results of both analyses (routine and triage) are summarized in Table 4.

Table 4. Estimation of the dose administered to the unknown samples.

Dose delivered (Gy)	Binucleated cells	Total MN	Cell distribution according to the number of micronuclei					ing	Estimated dose	Lower confidence	Upper confidence	Z-
			0	1	2	3	4	5	(Gy)	interval 95% (Gy)	interval 95 % (Gy)	score
1.5	1059	286	928	114	13	4	0	0	1,38	0,88	1,93	-1.2
	279	41	244	30	4	1	0	0	1,42	0,66	2.26	-0.8
3	1037	286	802	193	35	6	0	1	2,65	2,14	3,22	-1.75
	207	73	147	49	9	2	0	0	3,23	2,42	4,33	1.15



Both the routine analysis and triage analysis yielded dose estimates that were close to the actual delivered doses, with all z-scores within the acceptable range of |z| < 3, indicating that the results meet the performance criteria and that no corrective action is necessary under the fitness-for-purpose requirements outlined in ISO 13528:2022 [22]. As expected, confidence intervals were narrower in the full analysis compared to triage, reflecting greater precision when analyzing 1000 BN cells. The results confirm that both analysis modalities provide reliable dose estimations using automated CBMN scoring. While the full analysis provides greater precision, the triage approach yields dose estimates within acceptable error margins and significantly reduces analysis time. These results support the use of triage analysis in high-throughput settings and radiological emergencies, where rapid response is critical and a minor reduction in precision is tolerable.

Nevertheless, automated MN scoring is not without challenges. Misclassification of overlapping nuclei, sensitivity to staining quality, and residual overdispersion in MN counts point to areas requiring further optimization—such as improved cytoplasmic segmentation algorithms and standardized fixation protocols [5].

Automated algorithms are not infallible. Studies report non-negligible false-positive and false-negative rates for MN detection. For instance, one evaluation using MNScore module in Metafer 4 found that 0.7–2.2% of cells selected as BN were artifacts, and about 1.0% of detected micronuclei were false positives. False negatives were even higher (on average ~3.5%) because faint or small MN were missed. Importantly, these error rates tended to increase with radiation dose, likely due to cell debris and apoptosis confusing the software [25].

Semi-automated methods combine automated scanning with human review. Typically, the slide is scanned and candidate BN cells (and MN within them) are selected by software, and then a trained scorer inspects those selections to remove errors. This method enables the integration of staining variations and additional cellular markers that fully automated systems may fail to detect or accurately interpret, thereby enhancing



analytical flexibility and depth [26]. In some instances, semi-automated methods can outperform fully automated approaches by identifying errors that automated systems may overlook. Although this requires additional time and expert oversight, the improvement in accuracy is often significant. Inter-laboratory comparisons have recommend incorporating a manual verification step within automated scoring workflows to ensure high reliability and precision [27], [28].

4. CONCLUSIONS

Integrating automated microscopy with advanced statistical modeling offers substantial improvements in BD's standardization, reliability, and accuracy. Automated systems streamline the scoring process and minimize inter-analyst variability by applying consistent criteria for identifying micronuclei across large datasets. In this study, data obtained from over 82000 BN lymphocytes irradiated with X-rays revealed a dose-dependent increase in MN frequency, accompanied by increasing variance and a greater proportion of cells containing multiple MNs at higher doses.

Analysis of dispersion statistics demonstrated significant deviations from Poisson assumptions, with overdispersion across dose levels. These findings indicate that MN formation is not purely stochastic, likely reflecting biological heterogeneity and differential cellular radiosensitivity. To account for this overdispersion, an NB1 model was implemented, providing a superior fit compared to the Poisson model, as evidenced by lower residual deviance, reduced AIC, and higher log-likelihood values. The NB1 model's assumption of a variance linearly related to the mean was consistent with the empirical data, and all estimated parameters were statistically significant.

The resulting dose–response curve exhibited a clear linear–quadratic relationship, enabling accurate dose estimations for two blinded samples. The estimated doses and their



corresponding confidence intervals closely aligned with the actual delivered doses, demonstrating the reliability of the model. All z-scores remained within the acceptable range (|z| < 3), under criteria for fitness-for-purpose. These findings underscore the value of integrating automated scoring technologies with statistically robust models to enhance the precision and reproducibility of cytogenetic biodosimetry, particularly in scenarios that demand high-throughput analysis and rapid decision-making, such as radiological emergencies or population-wide exposure assessments.

Automated CBMN scoring systems have revolutionized biodosimetry by enabling high-throughput, objective analysis. Their advantages in speed and consistency make them invaluable for rapid response. Yet, they are not error-free: studies document nonzero false-positive and false-negative rates, especially under suboptimal conditions. Additionally, high-throughput automated systems require expensive hardware (motorized microscopes, cameras) and software licenses. They also demand calibration and maintenance. Therefore, these practical factors limit their deployment.

Semi-automated workflows address many of these shortcomings by adding visual quality control, yielding much higher specificity and more accurate dose estimates. In practice, a mixed approach is often optimal: use full automation to scan and roughly identify exposed individuals, then apply semi-automated review for detailed dose assessment. Awareness of the limitations of each method, and continual improvements in algorithms and imaging, will further enhance the reliability of automated biodosimetry [25].

Future work should focus on inter-laboratory harmonization of automated workflows, expansion of calibration curves for complex exposure scenarios (e.g., partial-body or protracted irradiation), and integration with complementary biomarkers (e.g., nucleoplasmic bridges, centromere FISH) to enhance dose reconstruction accuracy [5].



ACKNOWLEDGEMENTS

We want to acknowledge the work of Luisa Valle-Bourrouet and Isabel Castro Volio (R.I.P.), who were pioneers in radiation biology research in Costa Rica.

FUNDING

This research was made possible through the financial support of the Vice-Rectorate of Research at the University of Costa Rica and the International Atomic Energy Agency. The latter institution donated the Metasystems Metafer automated microscopy equipment used in this study.

CONFLICT OF INTEREST

The authors declare that they have no known competing financial interests or personal relationships that could have appeared to influence the work reported in this paper.

REFERENCES

- [1] Sommer, S., I. Buraczewska, and M. Kruszewski, "Micronucleus assay: The state of art, and future directions," Int J Mol Sci, vol. 21, no. 4, 2020, doi: 10.3390/ijms21041534.
- [2] Vral, A., M. Fenech, and H. Thierens, "The micronucleus assay as a biological dosimeter of in vivo ionising radiation exposure," Mutagenesis, vol. 26, no. 1, pp. 11–17, 2011, doi: 10.1093/mutage/geq078.
- [3] International Atomic Energy Agency, "Cytogenetic Dosimetry: Applications in Preparedness for and Response to Radiation Emergencies," Vienna, 2011. [Online]. Available: http://www-ns.iaea.org/standards/



- [4] Tucker, J. D., M. Vadapalli, M. C. Joiner, M. Ceppi, M. Fenech, and S. Bonassi, "Estimating the Lowest Detectable Dose of Ionizing Radiation by the Cytokinesis-Block Micronucleus Assay," Radiat Res, vol. 180, no. 3, pp. 284–291, Sep. 2013, doi: 10.1667/RR3346.1.
- [5] Tamizh Selvan, G. and P. Venkatachalam, "Potentials of cytokinesis blocked micronucleus assay in radiation triage and biological dosimetry," Journal of Genetic Engineering and Biotechnology, vol. 22, no. 4, p. 100409, Dec. 2024, doi: 10.1016/j.jgeb.2024.100409.
- [6] Beinke, C., M. Port, and M. Abend, "Automatic versus manual lymphocyte fixation: impact on dose estimation using the cytokinesis-block micronucleus assay," Radiat Environ Biophys, vol. 54, no. 1, pp. 81–90, Mar. 2015, doi: 10.1007/s00411-014-0575-0.
- [7] Rodrigues, M., L. Beaton-Green, R. Wilkins, and M. Fenech, "The potential for complete automated scoring of the cytokinesis block micronucleus cytome assay using imaging flow cytometry," Mutation Research/Genetic Toxicology and Environmental Mutagenesis, vol. 836, pp. 53–64, 2018, doi: https://doi.org/10.1016/j.mrgentox.2018.05.003.
- [8] Asano, N., Y. Katsuma, H. Tamura, N. Higashikuni, and M. Hayashi, "An automated new technique for scoring the rodent micronucleus assay: computerized image analysis of acridine orange supravitally stained peripheral blood cells," Mutation Research/Fundamental and Molecular Mechanisms of Mutagenesis, vol. 404, no. 1–2, pp. 149–154, Aug. 1998, doi: 10.1016/S0027-5107(98)00108-0.
- [9] Stich, H. F., A. B. Acton, and B. Palcic, "Towards an Automated Micronucleus Assay as an Internal Dosimeter for Carcinogen-Exposed Human Population Groups," 1990, pp. 94–105. doi: 10.1007/978-3-642-84068-5_7.
- [10] Varga, D., "An automated scoring procedure for the micronucleus test by image analysis," Mutagenesis, vol. 19, no. 5, pp. 391–397, Sep. 2004, doi: 10.1093/mutage/geh047.
- [11] Decordier, I. et al., "Automated image analysis of cytokinesis-blocked micronuclei: an adapted protocol and a validated scoring procedure for biomonitoring," Mutagenesis, vol. 24, no. 1, pp. 85–93, Sep. 2008, doi: 10.1093/mutage/gen057.
- [12] Thierens, H. and A. Vral, "The micronucleus assay in radiation accidents," Ann Ist Super Sanita, 2009.



- [13] Willems, P. et al., "Automated micronucleus (MN) scoring for population triage in case of large scale radiation events," Int J Radiat Biol, 2010, doi: 10.3109/09553000903264481.
- [14] Chaves-Campos, F.-A. et al., "Dose-effect calibration curve for high X-ray doses using the Calyculin-A chromosome premature condensation assay," Brazilian Journal of Radiation Sciences, vol. 12, no. 2, p. e2422, May 2024, doi: 10.15392/2319-0612.2024.2422.
- [15] González Mesa, J. E. et al., "LBDNet interlaboratory comparison for the dicentric chromosome assay by digitized image analysis applying weighted robust statistical methods," Int J Radiat Biol, vol. 100, no. 7, pp. 1019–1028, Jul. 2024, doi: 10.1080/09553002.2024.2356556.
- [16] International Atomic Energy Agency, "Absorbed dose determination in external beam radiotherapy: An international code of practice for dosimetry based on standards of absorbed dose to water (IAEA Technical Report Series No. 398)," 2000. Accessed: May 13, 2025. [Online]. Available: https://www.iaea.org/publications/6011/absorbed-dose-determination-in-external-beam-radiotherapy
- [17] Vargas-Segura W., Cordero-Ramírez A., and Avendaño-Soto E., "Procedure for calibration curve determination of radiochromic films for routine QA in Superficial Therapy X-Ray equipment," British Journal of Medical and Health Research, vol. 11, no. 06, 2024.
- [18] International Atomic Energy Agency, "Dosimetry of Small Static Fields Used in External Beam Radiotherapy An International Code of Practice for Reference and Relative Dose Determination," Vienna, 2017.
- [19] RStudio Team, "RStudio: Integrated Development for R." PBC, Boston, MA, 2020.
- [20] Hernández, A. et al., "Biodose Tools: an R shiny application for biological dosimetry," Int J Radiat Biol, vol. 99, no. 9, pp. 1378–1390, Sep. 2023, doi: 10.1080/09553002.2023.2176564.
- [21] Weiß, C. H., P. Puig, and B. Aleksandrov, "Optimal Stein-type goodness-of-fit tests for count data," Biometrical Journal, vol. 65, no. 2, Feb. 2023, doi: 10.1002/bimj.202200073.
- [22] International Organization for Standardization., "ISO 13528:2022: Statistical methods for use in proficiency testing by interlaboratory comparison.," 2022.



- [23] Bolognesi, C. et al., "Micronucleus test for radiation biodosimetry in mass casualty events: Evaluation of visual and automated scoring," Radiat Meas, 2011, doi: 10.1016/j.radmeas.2010.11.003.
- [24] Tamizh Selvan, G., N. K. Chaudhury, and P. Venkatachalam, "Comparison of results of the manual and automated scoring of micronucleus frequencies in 60Co-irradiated peripheral blood lymphocytes for triage dosimetry," Applied Radiation and Isotopes, vol. 97, pp. 70–77, 2015, doi: 10.1016/j.apradiso.2014.12.018.
- [25] Lee, Y., Y. W. Jin, K. M. Seong, R. C. Wilkins, and S. Jang, "Improving radiation dosimetry with an automated micronucleus scoring system: correction of automated scoring errors," Radiat Environ Biophys, vol. 62, no. 3, pp. 349–356, Aug. 2023, doi: 10.1007/s00411-023-01030-7.
- [26] Zaguia, N. et al., "A new tool for genotoxic risk assessment: Reevaluation of the cytokinesis-block micronucleus assay using semi-automated scoring following telomere and centromere staining," Mutation Research/Genetic Toxicology and Environmental Mutagenesis, vol. 850–851, p. 503143, Feb. 2020, doi: 10.1016/j.mrgentox.2020.503143.
- [27] Thierens, H. et al., "Is a semi-automated approach indicated in the application of the automated micronucleus assay for triage purposes?," Radiat Prot Dosimetry, vol. 159, no. 1–4, pp. 87–94, Jun. 2014, doi: 10.1093/rpd/ncu130.
- [28] Depuydt, J. et al., "RENEB intercomparison exercises analyzing micronuclei (Cytokinesis-block Micronucleus Assay)," Int J Radiat Biol, vol. 93, no. 1, pp. 36–47, Jan. 2017, doi: 10.1080/09553002.2016.1206231.

LICENSE

This article is licensed under a Creative Commons Attribution 4.0 International License, which permits use, sharing, adaptation, distribution and reproduction in any medium or format, as long as you give appropriate credit to the original author(s) and the source, provide a link to the Creative Commons license, and indicate if changes were made. The images or other third-party material in this article are included in the article's Creative Commons license, unless indicated otherwise in a credit line to the material. To view a copy of this license, visit http://creativecommons.org/ licenses/by/4.0/.